

CEBAF injector at 200 kV: K-Long bunch charge with spin flipper OFF/ON

Sunil Pokharel,^{a,*} Alicia Hofler,^b Reza Kazimi,^b Geoffrey Krafft,^{a,b} Max Bruker,^b Joe Games,^b Riad Suleiman^b and Shukui Zhang^b

^a*Center for Accelerator Science, Old Dominion University,
1026 W 47th Street, Norfolk, VA 23529, U.S.A.*

^b*Thomas Jefferson National Accelerator Facility,
12000 Jefferson Ave, Newport News, VA 23606, U.S.A.*

*E-mail: spokh003@odu.edu, hofler@jlab.org, kazimi@jlab.org,
krafft@jlab.org, brucker@jlab.org, games@jlab.org, suleiman@jlab.org,
shukui@jlab.org*

The forthcoming K-Long experiment in Jefferson Lab's Hall D presents distinct beam requirements, marked by a notably low bunch repetition rate and an unusually high bunch charge. Furthermore, the Continuous Electron Beam Accelerator Facility (CEBAF) Injector requires a parity quality beam for experiments such as the Measurement of a Lepton-Lepton Electroweak Reaction (MOLLER). In this study, to prepare for the upcoming K-Long experiment, using the optimized settings of the magnetic elements and RF amplitude and phases, we conducted simulations covering a range of bunch charge beams, from low to high specifications, while considering concurrent operations across all four Halls at CEBAF. Through these simulations, we systematically analyzed beam transmission as well as the transverse and longitudinal beam characteristics, examining the impact of Spin Flipper settings in both ON and OFF states.

*25th International Spin Physics Symposium (SPIN 2023)
24-29 September 2023
Durham, NC, USA*

*Speaker

1. Introduction

The Continuous Electron Beam Accelerator Facility (CEBAF) injector at Jefferson Lab provides beams to the main accelerator, consisting of two recirculating linacs operating at 1497 MHz and connected by beam transport arcs. These beams are then delivered to the experimental halls at frequencies of either 499 MHz or 249.5 MHz. For the K-Long experiment in Hall D, the baseline frequency for the CEBAF Photo-Injector Drive Laser is 15.59 MHz, with an additional desired frequency of 7.8 MHz [1]. Temporary solutions for the 15.6 MHz baseline are also explored [2] in the context of K-Long beam studies. The CEBAF polarized electron source employs a DC high-voltage photo-gun to generate spin-polarized electron beams. Notably, the electron beam itself comprises four interleaved components, produced using four lasers. This unique configuration allows for the simultaneous delivery of electron beams to four experimental halls [3]. Table 1 displays the experiments that will run concurrently with the K-Long experiment in different experimental halls and the associated average beam currents, repetition rates, and charge per bunch. However, for CEBAF operations, it is necessary to transmit both high and low-charge beams simultaneously through the injector, using the same injector optics. To meet the diverse beam requirements of the different halls, computer modeling is utilized

Table 1: CEBAF beam specifications/requirements for simultaneous operation of four experiment halls at JLab.

Halls/ Experiment	Frequency Rate (MHz)	Avg. Beam Current (μ A)	Bunch Charge (pC)	bunch spacing (ns)
Hall A (MOLLER)	249.5	65	0.26	4
Hall B	249.5	0.5	0.002	4
Hall C	249.5	35	0.12	4
Hall D (K-Long baseline)	15.6	5	0.32	64
Hall D (K-Long goal)	7.80	5	0.64	128

This paper represents a continuation and extension of the CEBAF injector modeling activities previously undertaken in [4, 5]. Specifically, our focus centers on the beam dynamics associated with the longitudinal and transverse beam characteristics of the upgraded injector, operating at a 200 kV DC gun, with attention to the spin-flipping states, both ON and OFF.

2. Theoretical Background

A Wien filter is a device featuring static electric and magnetic fields oriented orthogonally, strategically arranged to induce a net spin rotation without altering the beam's trajectory. Within the Continuous Electron Beam Accelerator Facility (CEBAF) injector, there are two Wien filter systems [6, 7], each accompanied by two spin flipper solenoid magnets positioned in between them to achieve the necessary spin orientations for the experimental target, as illustrated in Fig. 1. The polarization of the electron beam, originating from the photocathode, is longitudinal. The first Wien filter, situated downstream of the DC photo-gun, is oriented vertically and facilitates the

rotation of polarization from longitudinal to vertical. Subsequently, the second Wien filter, oriented horizontally, rotates the polarizations in-plane to counteract the precession induced by CEBAF transport magnets. The solenoids placed in between these filters ensure additional polarization rotations.

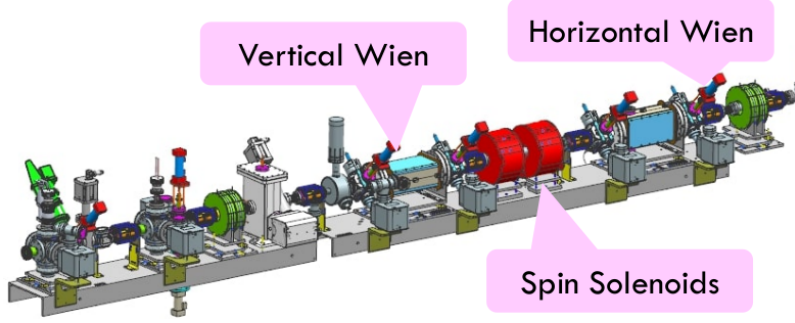


Figure 1: A schematic of the Spin Flipper setup in the CEBAF injector, comprising the Wien System and spin-flipping solenoids.

In the laboratory frame, the spin precession of a relativistic particle in an external electromagnetic field is described by the Thomas-BMT equation [8, 9]. For the CEBAF Spin Rotator, utilizing the Thomas-BMT equations, the spin precession relative to the electron momentum is expressed as:

$$\frac{d\vec{S}}{dt} = \Delta\vec{\Omega} \times \vec{S}, \quad \Delta\vec{\Omega} = \vec{\Omega}_s - \vec{\Omega}_{mom} \quad (1)$$

Here, the spin precession frequency, $\Delta\vec{\Omega}$, is given by:

$$\Delta\vec{\Omega} = -\frac{q}{m} \left[a\vec{B}_\perp + \frac{1}{\gamma}(1+a)\vec{B}_\parallel - \left(a - \frac{1}{\gamma^2 - 1} \right) \frac{\vec{\beta} \times \vec{E}}{c} \right] \quad (2)$$

In this equation, \vec{S} represents the spin vector of the particle in the rest frame, \vec{B}_\perp and \vec{B}_\parallel are the transverse and longitudinal components of the magnetic field in the laboratory frame relative to the velocity $\vec{\beta}c$ of the particle, and $\gamma = \sqrt{1 - \beta^2}$ is the Lorentz factor. The electric field is denoted by \vec{E} , and $a = (g - 2)/2$ is the anomalous gyromagnetic g-factor. For an electron with $q = -e$, the spin precessions in the Wien and solenoid are given by:

$$\text{Spin Precession in Wien: } \Delta\vec{\Omega} = \frac{e}{m} \left[a\vec{B}_\perp + \left(\frac{1}{\gamma^2 - 1} - a \right) \frac{\vec{\beta} \times \vec{E}}{c} \right] \quad (3)$$

$$\text{Spin Precession in Solenoid: } \Delta\vec{\Omega} = \frac{e}{m} \left[\frac{1}{\gamma}(1+a)\vec{B}_\parallel \right] \quad (4)$$

The spin precession frequency, $\Delta\Omega$, and the corresponding spin rotation angle, θ , are related through the equation $\theta = \Delta\Omega T$, where $T = L_{eff}/(\beta c)$ and L_{eff} represents the effective length of the spin flipper. In the Wien system, E denotes the electric field magnitude perpendicular to the particle velocity $v_z = \beta c$. Longitudinal fields, such as those present in solenoids, are confined to the injector and part of the Wien filter system. The remaining injector solenoids are deliberately designed to be counter-wound, featuring two alternating reversed loops, providing focusing while

yielding a net zero spin precession. Figure 1 illustrates a schematic of the system employed at CEBAF.

For the Wien filter to function as a spin rotator, maintaining the trajectory of particles passing through the device is crucial. In the single-particle model, this is accomplished by ensuring that the contributions of the electric and magnetic fields to the total force are zero, thus satisfying the so-called "Wien condition":

$$E_y = -v_z B_x \quad (5)$$

Here, E_y represents the vertical electric field, and B_x is the horizontal magnetic field for the vertical Wien filter. In the case of the horizontal Wien filter, the electric and magnetic fields are interchanged. Employing this mathematical framework allows for the determination of electric and magnetic field magnitudes corresponding to the desired spin rotation angle, applicable for operations within the range of -100 to +100 degrees for a 200 keV electron.

3. Simulation Details

The layout of the upgraded CEBAF injector and the elements related to bunching and timing of the beam are illustrated in Fig. 2. A 200 kV load locked DC high-voltage photogun [10] is utilized to generate polarized electron beams. The injector utilizes a two-stage bunching mechanism (prebuncher and buncher) [11] and a three-slit chopper [12] to regulate four continuous wave beams. To control transverse emittance, four apertures with hole sizes ranging from 4.0 to 6.5 mm are placed along the beamline. To manipulate spin direction in the halls, a 2-Wien filter system [6] is utilized. Additionally, a 15-degree bend dipole is positioned near the cathode to facilitate normal incidence of the lasers on the photocathode. The newly constructed "booster" cryomodule [13], which comprises a 2-cell superconducting capture section and a 7-cell superconducting cavity, is used to accelerate the 200 keV beam to 6.2 MeV. After being accelerated by the booster cryomodule, the beams are further accelerated to 123 MeV using two full cryomodules before the injector chicane. The injector beamline contains 11 solenoids, including spin solenoids set for 45 degrees and 12 quadrupoles for transverse focusing, excluding the four Wien quads. These elements are incorporated into the injector General Particle Tracer (GPT) [14] model, while inactive elements such as correctors and beam monitor devices are treated as drift spaces. The 15-degree bend dipole is modeled by a straight drift space and Wiens are set to OFF first and then ON. The beamline used for optimizations and simulations spans from the gun to a point just before the first full cryomodule, which is located 30.0 meters away from the gun.

The initial phase space distributions in the model are assumed to follow a Gaussian distribution in t , x , y , p_x , and p_y , aligning with the laser profile. The average transverse beam size is $\sigma_x = \sigma_y = 0.55$ mm, and the laser pulse length (FWHM) is 45 ps. The transverse thermal emittance is given by $\epsilon_{n,\perp} = \sigma_{\perp} \sqrt{\frac{MTE}{mc^2}}$, as reported in Ref. [15], and is 0.1348 mm mrad for a mean transverse energy of 30.691 meV for the GaAs photocathode. To account for the space charge effect, the space charge3Dmesh algorithm[16] is incorporated.

The on-axis normalized fields for the beamline elements are depicted in Fig. 3. For the simulations, we utilized the optimized settings for RF and the magnetic elements of the injector with the spin flipper OFF. Initially, spin flipper OFF conditions involve VWien being OFF and spin-

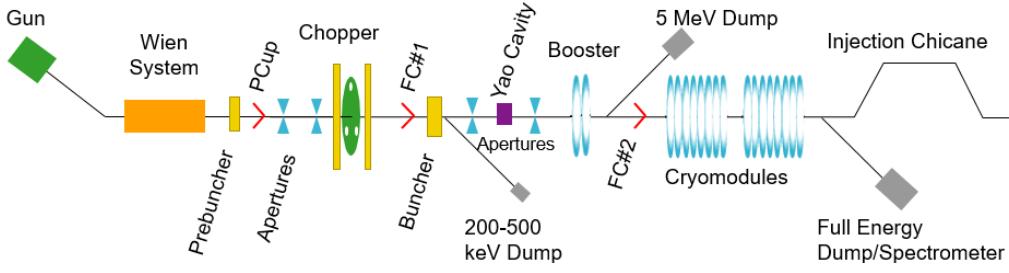


Figure 2: The CEBAF upgraded phase 2 full injector layout from the gun through the injection chicane merger into the entrance of the North Linac, Injector layouts, not to scale. Magnet elements are not shown. PCup, FC#1, and FC#2 are insertable Faraday cups.

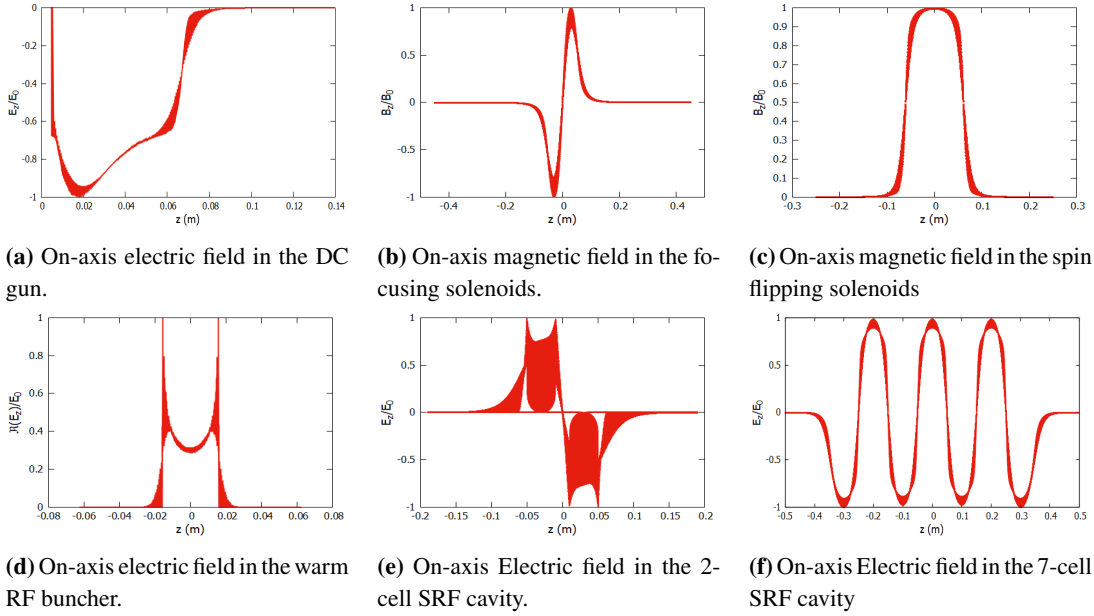


Figure 3: On-axis electric and magnetic for: (a) the high voltage DC gun at 200 kV, (b) Counterwound Focusing solenoids for low energy beam at different locations, (c) the spin flipping solenoids in between the Wien system, (e) the warm RF buncher cavity, (f) the 2-cell SRF cavity (f) the seven cell SRF cavity.

flipper solenoids, namely MFG1I04A and MFG1I04B, with \sum FGs = 0 degrees. Subsequently, for simulations with Spin flipper ON, VWien is set to ON (∓ 90 degrees) for left or right spin-flipping, and spin flipper solenoid conditions are set with \sum FGs = 90 degrees. The number of macroparticles used in the simulation is 10 k.

4. Results

In this section, we present the simulated beam characteristics along the beamline and upstream of the first full cryomodules, 30.0 m downstream of the 200 kV DC gun, after setting up simulations with spin flipper OFF/ON.

Table 2 presents the simulated beam characteristics of the CEBAF injector upstream of the first full cryomodules with spin flipper OFF. The results demonstrate that the bunch length is consistently

less than 1.1 ps upstream of the full modules, irrespective of the charge per bunch. The energy spread for all charge cases is approximately 1.4% or less. Additionally, the beam transmission along the beamline for different bunch charges indicates that the transmission exceeds 94.4% for all charges. The normalized emittance is less than 0.85 mm mrad for all charge configurations. It is worth noting that the average beam kinetic energy remains almost constant at around 6.98 MeV for all charge cases and spin OFF and ON scenarios, although this information is not shown in the table.

Table 2: Simulated beam characteristics upstream of the first full cryomodules with spin flipper OFF.

Beam Characteristics	Bunch Charge Specifications				
	2 fC	0.12 pC	0.26 pC	0.32 pC	0.64 pC
beam transmission (%)	99.52	94.40	97.84	99.28	95.75
bunch length (ps)	1.12	0.55	0.37	0.38	0.67
$\epsilon_{nx}, \epsilon_{ny}$ (mm mrad)	0.84, 0.42	0.27, 0.29	0.20, 0.25	0.21, 0.29	0.26, 0.32
σ_x, σ_y (mm)	1.86, 3.36	1.39, 1.53	1.04, 1.55	1.08, 1.68	1.30, 1.85
$\frac{\sigma_{E_k}}{E_k}$ (%)	1.40	0.65	0.63	0.69	1.04

Table 3 illustrates the simulated beam characteristics of the CEBAF injector upstream of the first full cryomodules with spin flipper ON. There is no significant difference in the beam characteristics between spin flip left and right. The results reveal that the bunch length is consistently less than 1.21 ps upstream of the full modules, regardless of the charge per bunch. The energy spread for all charge cases is approximately 1.5% or less. Furthermore, the beam transmission along the beamline for different bunch charges indicates that the transmission exceeds 96.61% for all charges. The normalized emittance is less than 0.78 mm mrad for all charge configurations.

Table 3: Simulated beam characteristics upstream of the first full cryomodules with spin flipper ON that mean flip left or right.

Beam Characteristics	Bunch Charge Specifications				
	2 fC	0.12 pC	0.26 pC	0.32 pC	0.64 pC
beam transmission (%)	99.95	96.61	99.93	97.96	99.89
bunch length (ps)	1.21	0.63	0.38	0.37	0.70
$\epsilon_{nx}, \epsilon_{ny}$ (mm mrad)	0.78, 0.32	0.29, 0.29	0.27, 0.29	0.23, 0.27	0.35, 0.42
σ_x, σ_y (mm)	1.70, 2.53	1.29, 1.52	1.08, 1.58	0.96, 1.53	1.23, 2.07
$\frac{\sigma_{E_k}}{E_k}$ (%)	1.50	0.70	0.67	0.74	1.16

From the simulations, it is observed that both with spin flipper OFF and ON cases, the beam transmission and beam characteristics upstream of the first full cryomodules meet the criteria for acceptable beam performance in the context of CEBAF injector operations.

Figure 4 illustrates the comparison of the variation of horizontal beam sizes along the beamline for different charge per bunch values in various experimental halls with both spin ON and OFF. The variation in bunch length and energy spread along the beamline for different bunch charge

specifications with spin flipper ON and OFF is shown in Figs. 5 and 6, respectively. The results indicate that there is no significant difference in the beam characteristics along the beamline of the CEBAF injector with spin flipper ON and OFF.

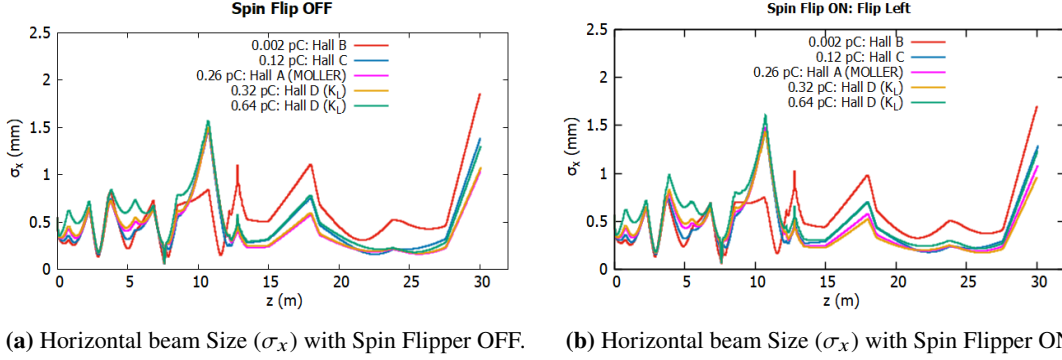


Figure 4: Horizontal beam sizes for different bunch charge specifications along the CEBAF injector beamline.

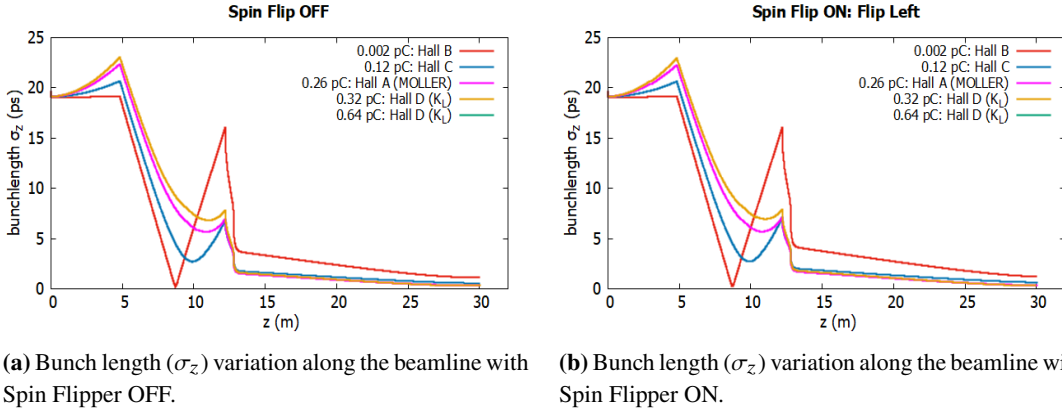


Figure 5: Bunch length variation along the beamline of the CEBAF injector for different bunch charge specifications.

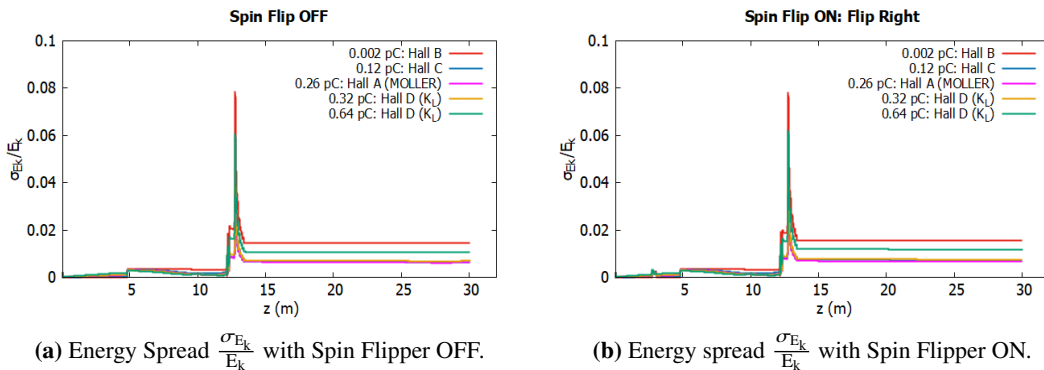


Figure 6: Energy spread for different bunch charge specification along the CEBAF injector beamline.

5. Outlook and future work

The CEBAF Injector simulation, incorporating VWien and spin solenoids, investigated the impact of spin manipulation on beam transmission and characteristics. Results reveal optimal transmission and beam quality at double the K-Long bunch charge baseline. The simulations also suggest that, with high charge settings, simultaneous operation with Halls A, B, C, and D is feasible, with minor differences in transverse beam optics when the Spin flipper is OFF or ON (spin flip left or spin flip right).

Despite the initially planned 200 kV DC gun voltage for the 2023 injector operation, it operated at 180 kV for three months in the Fall of 2023 due to a DC gun tripping incident in December. The current gun voltage is 140 kV, setting the stage for potential adjustments to 200 kV for the 2024 injector operations. Activating both horizontal and vertical Wiens, along with the Spin flipper at this voltage, will aid in assessing the compatibility of the MOLLER on the K-Long experiment.

Acknowledgments

Numerous individuals, both current and past members affiliated with Jefferson Lab, have contributed field maps, responded to inquiries, and offered guidance throughout the creation of these GPT models. The following is a partial list of contributors: K. Beard, J. Benesch, F. Hannon, F. Marhauser, G. Palacios-Serrano, M. Tiefenback, H. Wang, S. Wang, B. Yunn, and Y. Zhang. We express sincere appreciation for their valuable assistance.

This work was supported by the United States Department of Energy, Office of Science, Office of Nuclear Physics under contract No. DE-AC05-06OR23177.

References

- [1] M. Amaryan et al., *Strange hadron spectroscopy with secondary K_L beam in hall D*, *arXiv:2008.08215 [nucl-ex]* (2021).
- [2] S. Zhang, *Status of the CEBAF photo-injector drive laser system fo KLong Beam* https://wiki.jlab.org/klproject/images/8/8b/KLong_meeting_talk_Zhang.pdf
- [3] R. Kazimi, “Simultaneous Four-hall Operation for 12 GeV CEBAF”, in Proc. IPAC’13, Shanghai, China, May 2013, paper THPFI091, pp. 3502–3504.
- [4] A. Hoffer, *et al.*, “Modeling for the phased injector upgrade for 12 GeV CEBAF” in Proc. IPAC’23, Venice, Italy, May 2023, pp. 3280–3283. doi:10.18429/JACoW-IPAC2023-WEPL075
- [5] S. Pokharel *et al.*, “CEBAF Injector for K_L Beam Conditions”, in Proc. IPAC’22, Bangkok, Thailand, Jun. 2022, pp. 580–583. doi:10.18429/JACoW-IPAC2022-MOPOTK052
- [6] J. M. Grames *et al.*, “Two Wien Filter Spin Flipper”, in Proc. PAC’11, New York, NY, USA, Mar.-Apr. 2011, paper TUP025, pp. 862–864.

- [7] G. Palacios-Serrano, *et al.*, “ High voltage design and evaluation of Wien Filter for the CEBAF 200 keV injector upgrade ”, in *Proc.IPAC’21*, Campinas, SP, Brazil. doi : 10.18429/JACoW-IPAC2021-MOPAB324
- [8] J. D. Jackson, *Classical electrodynamics*, New York, NY, USA: Wiley, 1975.
- [9] S.Y. Lee, *Spin dynamics and snakes in Synchrotron*, River Edge, NJ USA: World Scientific, 1997
- [10] P. Adderley *et al.*, “Load-locked dc high voltage GaAs photogun with an inverted-geometry ceramic insulator”, *Phys. Rev. Spec. Top. Accel. Beams*, vol. 13, p. 010101, 2010. doi: 10.1103/PhysRevSTAB.13.010101
- [11] R. Kazimi *et al.*, “Injection Options for 12 GeV CEBAF Upgrade”, in *Proc. PAC’05*, Knoxville, TN, USA, May 2005, paper WPAP046.
- [12] R. Abbott *et al.*, “Design, Commissioning, and Operation of the Upgraded CEBAF Injector”, in *Proc. of the 1994 Linac Conf.*, Newport News, VA, USA, 1994, pp. 777–779.
- [13] R. Kazimi, A. Freyberger, F. E. Hannon, A. S. Hoffer, and A. Hutton, “Upgrading the CEBAF Injector with a New Booster, Higher Voltage Gun, and Higher Final Energy”, in *Proc. IPAC’12*, New Orleans, LA, USA, May 2012, paper TUPPR055, pp. 1945–1947.
- [14] Pulsar Physics, General Particle Tracer,
<http://www.pulsar.nl/gpt/>
- [15] I. V. Bazarov *et al.*, “Thermal emittance and response time measurements of negative electron affinity photocathodes”, *J. Appl. Phys.*, vol. 103, p. 054901, 2008.
doi:10.1063/1.2838209
- [16] S. B. Van Der Geer, *et al.* "3D space-charge model for GPT simulations of high brightness electron bunches." Institute of Physics Conference Series. Vol. 175. 2005.